Proc. Natl. Acad. Sci. USA
Vol. 79, pp. 390–394, January 1982
Biophysics

Location of monovalent cation binding sites in the gramicidin channel

(¹³C-enriched gramicidin A/¹³C NMR/phospholipid-packaged channels/ion-induced carbonyl carbon chemical shifts)

D. W. URRY, K. U. PRASAD, AND T. L. TRAPANE

Laboratory of Molecular Biophysics, University of Alabama in Birmingham, Birmingham, Alabama 35294

Communicated by Michael Kasha, September 14, 1981

ABSTRACT Six syntheses of gramicidin A have been carried out, each with 90% ^{13}C enrichment of a single carbonyl carbon these being the formyl, Val-1, Trp-9, Trp-11, Trp-13, and Trp-15 carbonyl carbons. Each gramicidin A was incorporated as the channel state into phospholipid structures, and the chemical shift of the carbonyl carbon resonance was monitored by ^{13}C NMR as a function of ion concentration. Plots of Na^+- and Tl^+-induced chemical shifts as a function of carbonyl location in the channel indicate two symmetrically related binding sites centered at the tryptophan carbonyls and separated by 23 Å. The absence of ion-induced chemical shifts for the formyl and Val-1 carbonyl carbon resonances indicates that there is no binding site midway through the channel but rather a central free-energy barrier for ion transit through the channel.

Ion-induced chemical shifts of the tryptophan carbonyl carbon resonances at 100 mM Na^+ verify that the tight binding constant ($K_b^t \simeq 70\ M^{-1}$), observed with ^{23}Na NMR, results from binding within the channel. This observation and the lateral, triangular distribution of the coordinating Trp-9, -11, and -13 carbonyls combine to provide an experimental demonstration that the carbonyls of the walls of the channel directly coordinate the ion, successfully competing with the polar solvent. With the binding sites verified and localized, it is possible to conclude that the transport mechanism for Na^+ is well represented by the case of the two-site model [D. W. Urry, Venkatachalam, C. M., Spisni, A., Läuger, P. & Khaled, M. A. (1980) *Proc. Natl. Acad. Sci. USA* 77, 2028–2032].

It is now well accepted (1–3) that the molecular structure of the gramicidin transmembrane channel is as first proposed in this journal in 1971 (4, 5). As demonstrated with space-filling models in Fig. 1, two monomers of gramicidin A (6, 7),

1 2 3 4 5 6 7 8

HCO-L-Val-Gly-L-Ala-D-Leu-L-Ala-D-Val-L-Val-D-Val-

9 10 11 12 13 14 15

L-Trp-D-Leu-L-Trp-D-Leu-L-Trp-D-Leu-L-Trp-$HNCH_2CH_2OH$,

each in the single-stranded $\beta_{3,3}^{6,3}$-helical conformation (5, 8–12), associate formyl end to formyl end by means of six intermolecular hydrogen bonds. As such, the channel has a 2-fold symmetry axis perpendicular to the channel (helix) axis. The diameter of the channel is 4 Å, and the channel length is 25 Å (Trp-11 oxygen to Trp-11 oxygen) to 30 Å (Trp-15 oxygen to Trp-15 oxygen).

Interest in the gramicidin channel arises for many reasons. It is the first ion-selective transmembrane channel of known molecular structure that is essentially impermeable to anions and multivalent cations and has substantial selectivity among monovalent cations (13); it exhibits high single-channel ion fluxes—e.g., 10^7 Na^+ per sec at 25°C, 100 mV, and 1 M NaCl (14, 15)—giving a single-channel conductance of the order of 10 pS, which is similar to that of physiological channels (16); and it exhibits many additional and more subtle features similar to those of physiological channels, such as concentration dependence of permeability ratios, saturation effects (and even maxima) in conductance on increasing ion concentration, monovalent cation-competition and -blocking effects (17–19), divalent cation damping of single-channel currents (20), and multivalent anion-screening effects (21).

Qualitatively, the mechanism of ion transport and of selectivity has been described as arising from a libration of peptide

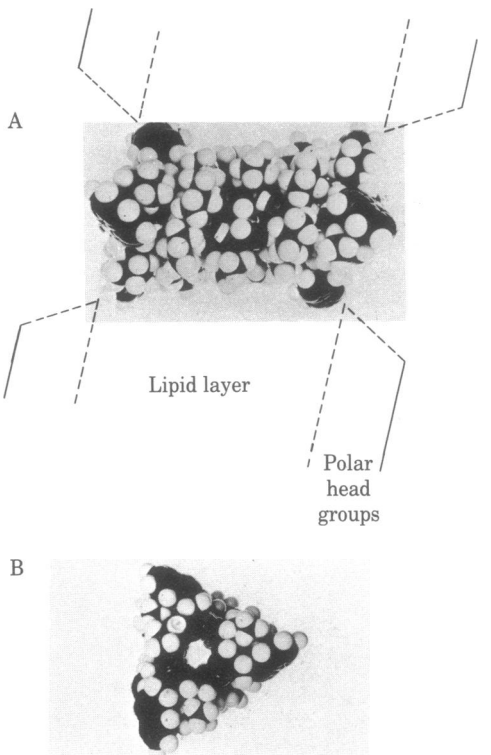

FIG. 1. Space-filling model of the gramicidin A transmembrane channel. (*A*) Side view looking along the 2-fold symmetry axis of the structure comprised of two helical monomers associating formyl end to formyl end by six intermolecular hydrogen bonds and depicted as spanning the lipid layer of a lipid bilayer. (*B*) Channel view showing a 4-Å-diameter channel and the tryptophan-11, -13, and -15 carbonyls directed outward into the aqueous solution.

The publication costs of this article were defrayed in part by page charge payment. This article must therefore be hereby marked "*advertisement*" in accordance with 18 U. S. C. §1734 solely to indicate this fact.

moieties, which allows the oxygen of the carbonyl to librate into the channel, lining it with partial negative charges, decreasing the diameter of the channel and providing for direct lateral coordination of the monovalent cation, which passes through the channel with two coordinate water molecules, one preceding and one following it through the channel (12). As there is no structural counterpart for moving the positive end of the peptide dipole moment into the channel, anions cannot enter. Furthermore, although the single wall of the helix with its carbonyls is viewed in this qualitative description as sufficient to lower the ion self-energy of a monovalent cation, it is considered to be insufficient to shield a divalent cation from the effects of the low-dielectric-constant lipid surrounding the channel (12, 22). As to ion occupancy of the channel, models of one-ion, two-ion, three-ion, and four-ion occupancy have been considered (23–28, 17, 18), but the uniqueness of even a set of rate constants for a given model has not been established (29). Accordingly, it is necessary to devise means of directly observing the ion locations within the channel to determine the correct occupancy model.

Recently it has been demonstrated that gramicidin A channels can be packaged in phospholipid structures (30, 31), that binding and rate constants can be determined by using ^{23}Na NMR (26, 27, 32), and that these constants can be used within the framework of Eyring rate theory for introducing voltage dependence to calculate the single-channel currents as a function of concentration and transmembrane potential (26, 27). Even so, it has not yet been possible to deduce unambiguously the number of binding sites in the channel. Again, completion of an understanding of the mechanism of channel transport is blocked by the lack of information on the number and location of the ion-binding sites within the channel. In the present report, binding sites are defined for Na^+ and Tl^+.

MATERIALS AND METHODS

^{13}C Enrichment of the Peptide Carbonyl Carbons of Gramicidin. Four syntheses of gramicidin A containing [1-^{13}C]Trp-9, [1-^{13}C]Trp-11, [1-^{13}C]Trp-13, or [1-^{13}C]Trp-15, respectively, were carried out by the solid-phase method. The details of synthesis of gramicidin A by this method and the verification of structure will be presented elsewhere. The indicated carbonyl carbons were enriched to 90% ^{13}C. The [*formyl*-^{13}C]- and [1-^{13}C]Val-1-containing gramicidins were prepared from natural gramicidin, in the former case by deformylation and reformylation with [^{13}C]formic acid and in the latter case by deformylation, removal of the Val-1 residue by Edman degradation, recoupling with 90% [1-^{13}C]Val-1, and reformylating. The natural gramicidin contains about 70% gramicidin A, 10% gramicidin B and 20% gramicidin C. Residue 11 is Phe for gramicidin B and Tyr for gramicidin C. All six products were verified by ^{13}C NMR spectra, circular dichroism spectra, and by high-performance reverse-phase liquid chromatography.

Phospholipid Packaging of Gramicidin Channels. Each ^{13}C-enriched gramicidin was incorporated into phospholipid structures comprised of L-α-lysolecithin (Avanti Biochemicals; lot no. LPC-18) by heating at 70°C for 20 hr in the presence of 0.5 mM NaCl as described (30, 31). The circular dichroism spectra of [1-^{13}C]Val-1-containing natural gramicidin and [1-^{13}C]Trp-11-containing gramicidin A are shown in Fig. 2 (curves a and b), where the curves are seen to superimpose perfectly except for small differences near 200 nm, which may arise due to the presence of some gramicidins B and C in the [1-^{13}C]Val-1-containing natural gramicidin. Seen as curve c is the gramicidin associated with lysolecithin micelles but not in the channel state. The nonchannel state represented by curve c is converted to the channel state represented by curves a and b by the extended heating at 70°C. In this state, ion interaction such as the ^{23}Na chemical shift at 0.5 mM NaCl and other properties satisfy the numerous criteria established as evidence of the channel state (30, 31, 33). The channel concentration was about 3 mM.

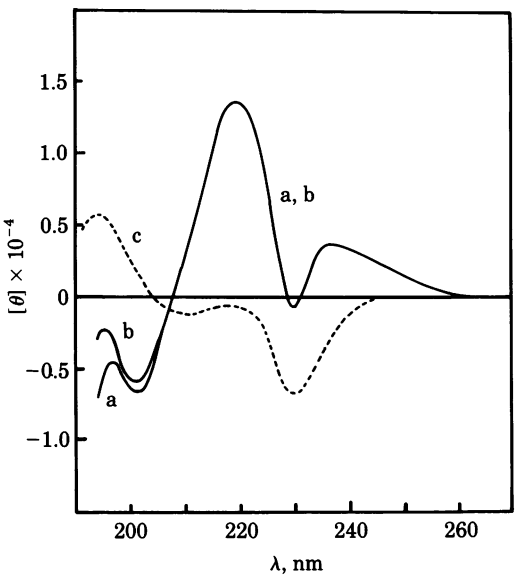

FIG. 2. Circular dichroism spectra of [1-^{13}C]Val-1-containing natural gramicidin (curve a), and [1-^{13}C]Trp-11-containing gramicidin A (curve b), with both having the spectrum characteristic of the channel state. Curve c is the spectrum obtained before heat incorporation into the lipid of the phospholipid. This state shows neither perturbation of the lipid layer, nor ion interactions; when in the state represented by curves a and b, the lipid layer becomes relatively immobilized, and the ion interactions exhibit a set of properties similar to those of the channel in the black lipid membrane studies.

^{13}C NMR. The ^{13}C NMR spectra were obtained at 70°C on a JEOL FX-100 instrument operating at 25 MHz. The reference ^{13}C NMR spectra were obtained in the presence of 0.5 mM NaCl. The sodium concentration was then raised to 100 mM, which is the concentration for optimizing single-ion occupancy based on binding constants, of about 50 M^{-1} for the tight site and 1 M^{-1} for the weak site, determined at this temperature. This is the concentration used for monitoring the chemical shift induced in the ^{13}C-enriched carbonyl C-1 resonance by Na^+. The next addition was 3.3 mM thallium acetate. With both the tight and weak binding constants for Tl^+ being about 2 orders of magnitude greater than for Na^+, (ref. 34; unpublished data), Tl^+ displaces Na^+ and, with Tl^+ and channels both about 3 mM, results in a ^{13}C carbonyl resonance chemical shift that approaches that of single-ion occupancy by Tl^+. Increasing the Tl^+ concentration to 83 mM gives the effect of approaching double occupancy on the carbonyl carbon chemical shift.

RESULTS

^{13}C NMR spectra for the Na^+-induced chemical shifts are seen in Fig. 3. As the lipid carbonyl carbon chemical shift is unchanged by any of the ion additions considered here, it can serve as a sharp nearby reference signal for the peptide carbonyl carbon resonance, which is much broader because of the limited mobility of the peptide backbone. Addition of 100 mM NaCl had no effect on the chemical shift of the formyl and Val-1 carbonyl carbon resonances (Fig. 3 *A* and *B*). Fig. 3*C* shows a very small chemical shift of the Trp-9 carbonyl carbon resonance, but in Fig. 3*D* there is a large shift, about 1 ppm, of the Trp-11 carbonyl carbon resonance on addition of 100 mM NaCl. A substantial shift is still apparent in Fig. 3*E* for the Trp-13 carbonyl

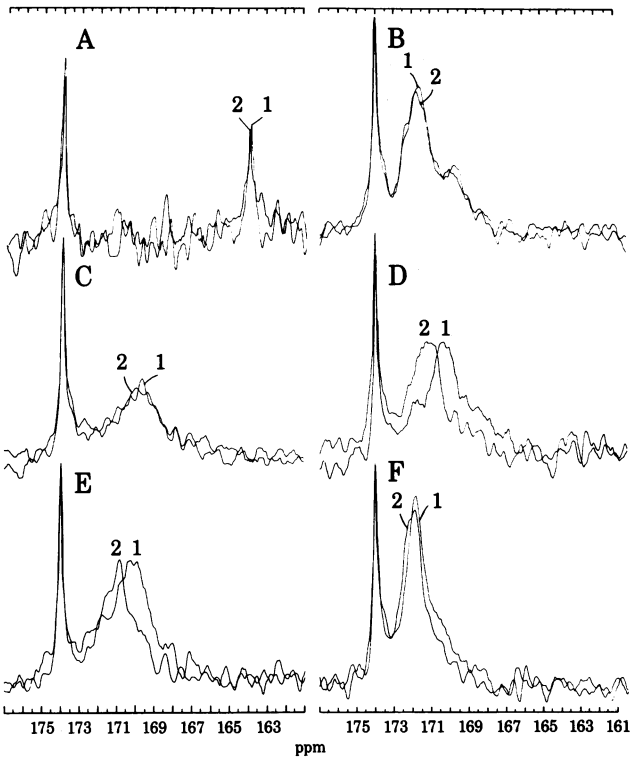

FIG. 3. ^{13}C NMR spectra of the carbonyl carbon region. Chemical shifts are given with respect to external hexamethyldisiloxane. The sharp peak at low field (174 ppm) is due to the unenriched lipid carbonyl carbon, and the broader peak at higher field is the ^{13}C resonance of the specified polypeptide backbone carbonyl carbon which has been enriched to 90%. In each case, a reference curve (labeled 1) is included in which the sodium ion concentration is 0.5 mM, and this curve is compared with that (labeled 2) obtained in the presence of 100 mM NaCl. (*A*) [1-^{13}C]Formyl-containing natural gramicidin showing no perturbation of the formyl carbonyl carbon resonance on raising the NaCl concentration. (*B*) [1-^{13}C]Val-1-containing natural gramicidin again showing no perturbation of the enriched carbonyl carbon resonance. (*C*) [1-^{13}C]Trp-9-containing gramicidin A showing little or no perturbation. (*D*) [1-^{13}C]Trp-11-containing gramicidin A showing a large, 1-ppm, downfield shift on increasing the NaCl concentration. (*E*) [1-^{13}C]Trp-13-containing gramicidin A showing a 0.8-ppm downfield shift. (*F*) [1-^{13}C]Trp-15-containing gramicidin A showing a 0.2-ppm downfield shift for 100 mM NaCl.

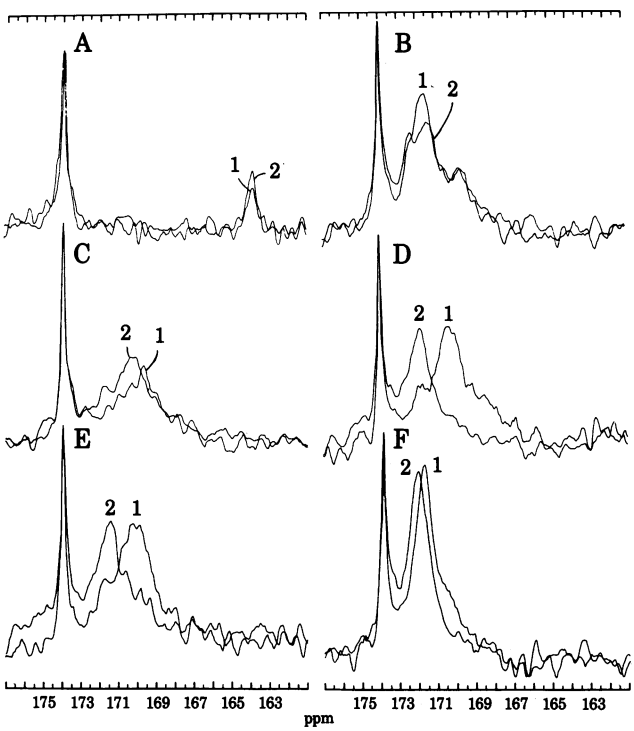

FIG. 4. ^{13}C NMR spectra of phospholipid-packaged gramicidin channels showing the carbonyl carbon region. Chemical shifts are given with respect to external hexamethyldisiloxane. The lipid carbonyl carbon resonance, which exhibits no shifting for any of the ion additions considered here, serves as a convenient sharp reference peak at 174 ppm. The spectra are compared for 0.5 mM NaCl (spectrum 1) and 83 mM thallium acetate (spectrum 2). (*A*) [1-^{13}C]Formyl-containing natural gramicidin showing no shifting of the formyl carbonyl carbon resonance on addition of Tl^+. (*B*) [1-^{13}C]Val-1-containing natural gramicidin showing no Tl^+-induced shifting of the Val-1 carbonyl carbon resonance. (*C*) [1-^{13}C]Trp-9-containing gramicidin A showing a 0.5-ppm Tl^+-induced chemical shift. (*D*) [1-^{13}C]Trp-11-containing gramicidin A showing a 1.6-ppm Tl^+-induced chemical shift. (*E*) [1-^{13}C]Trp-13-containing gramicidin A with a 1.2-ppm downfield shift on addition of 83 mM Tl^+. (*F*) [1-^{13}C]Trp-15-containing gramicidin A with a 0.3-ppm Tl^+-induced chemical shift.

carbon resonance. Thus, we were able to localize the Na^+-binding site to a position between the Trp-11 and Trp-13 carbonyl carbons. Due to an ion occupancy of $\approx$0.8–0.9 for the channel, the chemical shift for completely filling the channel (i.e., for double occupancy) would be greater than 2 ppm for the Trp-11 carbonyl carbon resonance.

^{13}C NMR spectra for the Tl^+-induced chemical shifts showed no discernible chemical shift of the formyl and Val-1 carbonyl carbon resonances on addition of 83 mM thallium acetate (Fig. 4 *A* and *B*). However, in the case of Tl^+, the Trp-9 carbonyl carbon resonance (Fig. 4) did show a significant ion-induced chemical shift (about 0.5 ppm). The chemical shift increased to 1.6 ppm for Trp-11 (Fig. 4*D*), then decreased somewhat for Trp-13, and became quite small again for Trp-15 carbonyl carbon resonances. Thus, again the monovalent cation-binding site was found to be localized between the Trp-11 and Trp-13 carbonyls. With the expected ion occupancy of about 1.6 ions per channel or about 0.8 per site, again a chemical shift of about 2 ppm for the most proximal carbonyl is the value that would result from complete occupancy.

The ion-induced chemical shifts of Figs. 3 and 4 were plotted (Fig. 5) as a function of position along the channel. In Fig. 5*A* are seen the locations of the carbonyl carbons and in Fig. 5*B* is the spatial distribution of the carbonyls seen in side view. With the 2-fold symmetry axis perpendicular to the channel axis, the six separate carbonyl carbon enrichments provide data on 12 locations distributed along the channel. With the point of view that the chemical shift in the carbonyl carbon resonance results from interactions at the carbonyl oxygen, the position of the carbonyl oxygen was plotted as a function of the ion-induced chemical shift in Fig. 5*C*. It is apparent that the cation binding for both Tl^+ and Na^+ is localized with two sites separated by about 23 Å and with no binding midway through the channel.

A comparison of the carbonyl carbon resonance chemical shifts induced by 3.3 mM and 83 mM Tl^+ is of interest because at low concentration the tight site would be saturated and at high concentration the weak site would be more than 50% occupied. Both the low and high concentrations of Tl^+ caused the largest shift in the Trp-11 carbonyl carbon resonance. For the incorporation of [1-^{13}C]Trp-11-containing gramicidin A, the actual channel concentration was 2.8 mM. With a tight binding constant of about $1 \times 10^3\ M^{-1}$ and a weak binding constant of about $50\ M^{-1}$ for Tl^+ (ref. 17; unpublished data), at 3.3 mM Tl^+ the channel occupancy would be 1.1–1.2 ions with essentially com-

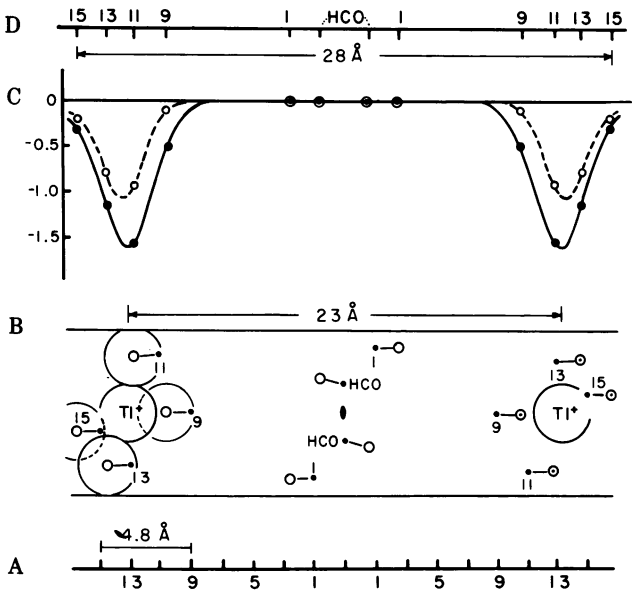

FIG. 5. Distribution of carbonyls in the gramicidin channel and plot of ion-induced chemical shifts. (*A*) Carbonyl carbon positions. (*B*) Spatial distribution of carbonyls in the gramicidin channel, including position of the Tl^+ ions. (*C*) Plot of cation-induced carbonyl carbon chemical shifts in ppm: δ (in absence of ion) − δ (in presence of ion). ●, Tl^+ binding (double occupancy; 83 mM); ○, Na^+ binding (single occupancy; 100 mM). (*D*) Carbonyl oxygen locations. Note that the formyl and Val-1 carbonyls are unperturbed by the presence of 100 mM Na^+ and 83 mM Tl^+, indicating that there is no appreciable ion occupancy in the central 7–8 Å of the channel. The plot in *C* shows the binding sites to be separated by 23 Å for Tl^+ and 24 Å for Na^+. The helix sense of the channel is taken to be left-handed (4, 5).

plete saturation of the tight site. The observed chemical shift was 1.1 ppm. At 83 mM Tl^+ the channel occupancy would be about 1.6, and the observed chemical shift was 1.6 ppm. Although it is fortuitous that the magnitude of the chemical shift coincided with the ion occupancy, the result demonstrates that the tight and weak sites are at the same location in the channel. These results are due to the 2-fold symmetry of the channel structure and the rapid exchange between sites with an observation frequency of 25 MHz.

DISCUSSION

Monovalent Cation Binding to Carbonyl Carbons. Enniatin B, a cyclohexadepsipeptide of alternating L and D residues with 3-fold symmetry, is an instructive cyclic correlate of the gramicidin-channel structure, which has 6.3 residues per turn and alternating L and D residues. The crystal structure of the Enniatin B–K^+ complex (35) shows the carbonyls pointing in alternate directions, parallel and antiparallel to the 3-fold molecular axis in analogy to the gramicidin-channel structure in which the carbonyls point parallel and antiparallel to the channel axis; of particular interest is that in the crystal structure of the Enniatin B–K^+ complex, the carbonyl oxygens directly coordinate the cation. This provides an opportunity to evaluate the ^{13}C chemical shifts expected with direct peptide carbonyl coordination of the bare cation.

In methanol solution, it has been demonstrated that formation of the Enniatin B–K^+ complex causes the peptide carbonyl carbon resonances to shift downfield 1.5 ppm (36). Thus, the observed ion-induced shifts, of the Trp-11 carbonyl carbon resonance of 1.0 ppm and 1.6 ppm for Na^+ and Tl^+, respectively, with the shift for full occupancy expected to be 2 ppm argue for direct coordination of the bare cation by the carbonyl oxygens. The lesser shifts shown by the other carbonyl carbons are due to their helical arrangement, placing them at somewhat larger distances from the cation. This situation is depicted in Fig. 6, which is an end-on view looking from the solution end of the channel, with the distances in Å of the Trp carbonyl oxygens from the midpoint of the channel given in parentheses. The double circle represents the mean position of the helical backbone atoms, and the peptide carbonyl oxygens are shown librated toward the helix axis as previously depicted for the libration mechanism (12). What Fig. 6 shows is that the Trp carbonyl oxygens surround the bare cation laterally, with room for water preceding and following the cation in the channel. An important point to be made is that the carbonyls of the channel are able to compete with water, even with the proximity of the membrane lipid, and to do so with binding constants of the order of 10^2 to 10^3 M^{-1}. Therefore, it is not required that more water be in the channel to increase the dielectric constant; the carbonyls themselves, when they have the proper orientation due to the local peptide conformation, can provide a greater free energy of solvation than water. This is consistent with the realization that, while the dielectric constant of water is about 80, the dielectric constant of *N*-methylacetamide, a model for the peptide moiety, is about 180 (37). This is also consistent with the NMR-observed chemical shifts. Whereas the carbonyl carbon resonances shift downfield on complexation with the cation because of a loss of electron density surrounding the carbonyl carbon, the resonance of the ^{23}Na nucleus on going from water into the channel shifts some 20 ppm upfield (26, 27), indicating the greater electron density accessible to the cation in the channel as compared to aqueous solution.

On the Location of the Binding Sites and the Magnitude of Ion–Ion Repulsion. While the structure of the cation-containing channel within a lipid membrane has not been determined by diffraction methods, a crystal structure of gramicidin A at low resolution has been obtained for the K^+ and Cs^+ complexes (3). The apparent length and diameters of the helical structure are within tenths of an Å of the channel structure described some 10 years ago (ref. 5; ref. 12, table of $\beta^6_{3,3}$ helix parameters). In the crystal structure, the cation-binding sites are seen to be within the end-to-end aligned helices and to recur with separations of 21 Å and 5 Å, but it is not possible to say whether this indicates two sites straddling the midpoint of the channel and separated by 5 Å or whether it is two sites separated by 21 Å

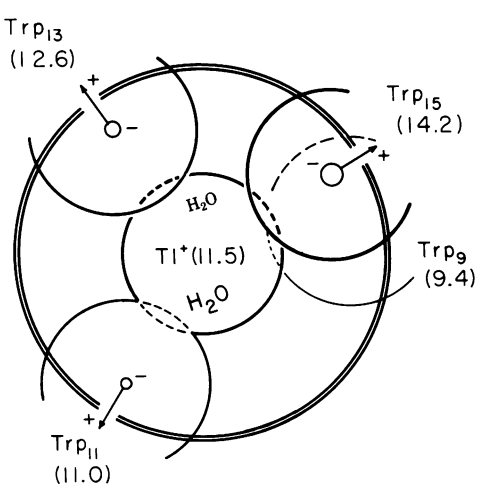

FIG. 6. Channel view from the aqueous solution as in Fig. 1*B*. Note that the carbonyl oxygens surround the monovalent cation. The numbers in brackets are the distance in Å from the 2-fold symmetry axis of the channel to the particular Trp oxygen.

and located near the entrance to the channel. If the crystal structure is relevant to the channel, then it can be expected on the basis of the data in Figs. 3, 4, and 5 that the latter is correct, and the refined crystal structure is awaited with interest to see whether the sites are as demonstrated here in phospholipid structures. The slightly greater distance of 23–24 Å between the two sites as reported here may be due to the proximity of the lipid and the greater flexibility near the end of the helical structure; it could be that it is more appropriate to plot the ion location with respect to the carbonyl carbon rather than the carbonyl oxygen, or it could be that the dipeptide repeat distance is closer to 1.5 Å than to 1.6 Å.

With the same location being observed for the tight site for Na^+ at 100 mM and Tl^+ at 3.3 mM as for the weak site which is largely occupied at 83 mM Tl^+, it is apparent that the sites are structurally identical and related by the 2-fold symmetry axis. This requires that the difference between binding constants arises from the repulsion experienced by the second ion due to the presence in the channel of the first ion. The best experimental estimates of the Na^+ binding constants for the malonyl-bis-desformyl-gramicidin channel (where the two monomers are covalently linked by a malonyl bridge between the NH_2-terminal amino groups), is $K_b^t \simeq 70\ M^{-1}$ and $K_b^w \simeq 1\ M^{-1}$ at 30°C (27). The repulsion is similarly reflected in the off rate constants, $k_{off}^t \simeq 3 \times 10^5$/sec and $k_{off}^w \simeq 2 \times 10^7$/sec (27). Thus, it appears that the free energy of repulsion, between two Na^+ separated 24 Å by a single file of water and laterally coordinated by carbonyls, is 2.5 kcal/mol. This gives a repulsion constant of about 60 kcal·Å/mol. It is interesting to note that similar differences between equivalent binding constants have been reported by Eisenman *et al.* in analyses of transport properties for both Tl^+ and K^+ (17, 34).

Although there is yet much to be completed for a thorough understanding of the mechanism of channel transport as exemplified by the gramicidin channel—such as the facilitated on rate for the second ion (26) and the dispersion of single-channel currents (unpublished data) that have been proposed to arise from changes in side-chain rotameric states altering the energetics of libration (38) and such as the rate constant for jumping between sites during single occupancy, which has been estimated in the case of Tl^+ by means of dielectric relaxation studies (39)—what is now defined for the first time is the location of two binding sites within a transmembrane channel and an estimate of the repulsion attending double occupancy.

The authors thank J. T. Walker for assistance in the syntheses and S. A. Romanowski for assistance in the NMR studies. This work was supported in part by National Institutes of Health Grant GM-26898.

1. Bamberg, E., Apell, H.-J. & Alpes, H. (1977) *Proc. Natl. Acad. Sci. USA* **74**, 2402–2406.
2. Weinstein, S., Wallace, B., Blout, E. R., Morrow, J. S. & Veatch, W. (1979) *Proc. Natl. Acad. Sci. USA* **76**, 4230–4234.
3. Koeppe, R. E., II, Berg, J. M., Hodgson, K. O. & Stryer, L. (1979) *Nature (London)* **279**, 723–725.
4. Urry, D. W. (1971) *Proc. Natl. Acad. Sci. USA* **68**, 672–676.
5. Urry, D. W., Goodall, M. C., Glickson, J. D. & Mayers, D. F. (1971) *Proc. Natl. Acad. Sci. USA* **68**, 1907–1911.
6. Sarges, R. & Witkop, B. (1964) *J. Am. Chem. Soc.* **86**, 1862–1863.
7. Gross, E. & Witkop, B. (1965) *Biochemistry* **4**, 2495–2501.
8. Ramachandran, G. N. & Chandrasekharan, R. (1972) in *Progress in Peptide Research*, Proceedings of the Second American Peptide Symposium, ed. Lande, S. (Gordon & Breach, New York), Vol. 2, 195–206.
9. Ramachandran, G. N. & Chandrasekharan, R. (1972) *Indian J. Biochem. Biophys.* **9**, 1–11.
10. Urry, D. W., Long, M. M., Jacobs, M. & Harris, R. D. (1975) *Ann. N.Y. Acad. Sci.* **264**, 203–220.
11. Urry, D. W. (1972) *Proc. Natl. Acad. Sci. USA* **69**, 1610–1614.
12. Urry, D. W. (1973) in *Conformation of Biological Molecules and Polymers*, The Jerusalem Symposia on Quantum Chemistry and Biochemistry, eds. Bergmann, E. D. & Pullman, B. (Israel Academy of Sciences, Jerusalem), Vol. 5, pp. 723–736.
13. Myers, V. B. & Haydon, D. A. (1972) *Biochim. Biophys. Acta* **274**, 313–322.
14. Bamberg, E., Kolb, H.-A. & Läuger, P. (1976) in *The Structural Basis of Membrane Function*, eds. Hatefi, Y. & Djavadi-Ohaniance, L. (Academic, New York), pp. 143–157.
15. Bamberg, E. & Läuger, P. (1974) *Biochim. Biophys. Acta* **367**, 127–133.
16. Urry, D. W. (1979) *Int. Rev. Neurobiol.* **21**, 311–334.
17. Eisenman, G., Sandblom, J. & Neher, E. (1977) in *Metal Ligand Interactions in Organic Chemistry and Biochemistry*, eds. Pullman, B. & Goldblum, N. (Reidel, Dordrecht, The Netherlands), Part 2, pp. 1–36.
18. Sandblom, J., Eisenman, G. & Neher, E. (1977) *J. Membr. Biol.* **31**, 383–417.
19. Neher, E. (1975) *Biochim. Biophys. Acta* **401**, 540–544.
20. Bamberg, E. & Läuger, P. (1977) *J. Membr. Biol.* **35**, 351–375.
21. Apell, H.-J., Bamberg, E., Alpes, H. & Läuger, P. (1977) *J. Membr. Biol.* **31**, 171–188.
22. Urry, D. W. (1978) *Ann. N.Y. Acad. Sci.* **307**, 3–27.
23. Läuger, P. (1973) *Biochim. Biophys. Acta* **311**, 423–441.
24. Hladky, S. B., Urban, B. W. & Haydon, D. A. (1979) in *Membrane Transport Processes*, eds. Stevens, C. F. & Tsien, R. W. (Raven, New York), Vol. 3, pp. 79–103.
25. Urban, B. W., Hladky, S. B. & Haydon, D. A. (1978) *Fed. Proc. Fed. Am. Soc. Exp. Biol.* **37**, 2628–2632.
26. Urry, D. W., Venkatachalam, C. M., Spisni, A., Läuger, P. & Khaled, M. A. (1980) *Proc. Natl. Acad. Sci. USA* **77**, 2028–2032.
27. Urry, D. W., Venkatachalam, C. M., Spisni, A., Bradley, R. J., Trapane, T. L. & Prasad, K. U. (1980) *J. Membr. Biol.* **55**, 29–51.
28. Hägglund, J., Enos, B. & Eisenman, G. (1979) *Brain Res. Bull.* **4**, 154–158.
29. Urry, D. W. (1981) in *Membranes and Transport*, ed. Martonosi, A. (Plenum, New York), in press.
30. Urry, D. W., Spisni, A., Khaled, M. A., Long, M. M. & Masotti, L. (1979) *Int. J. Quantum Chem. Quantum Biol. Symp.* **6**, 289–303.
31. Urry, D. W., Spisni, A. & Khaled, M. A. (1979) *Biochem. Biophys. Res. Commun.* **88**, 940–949.
32. Venkatachalam, C. M. & Urry, D. W. (1980) *J. Magn. Reson.* **41**, 313–335.
33. Masotti, L., Spisni, A. & Urry, D. W. (1980) *Cell Biophys.* **2**, 241–251.
34. Eisenman, G., Sandblom, J. & Neher, E. (1978) *Biophys. J.* **22**, 307–340.
35. Dobler, M., Dunitz, J. D. & Krajewski, J. (1969) *J. Mol. Biol.* **42**, 603–606.
36. Urry, D. W. (1976) in *Enzymes of Biological Membranes*, ed. Martonosi, A. (Plenum, New York), pp. 31–69.
37. Urry, D. W. (1978) *Ann. N.Y. Acad. Sci.* **307**, 3–27.
38. Urry, D. W., Venkatachalam, C. M., Prasad, K. U., Bradley, R. J., Parenti-Castelli, G. & Lenaz, G. (1981) *Int. J. Quantum Chem. Quantum Biol. Symp.* **8**, in press.
39. Henze, R., Neher, E., Trapane, T. L. & Urry, D. W. (1982) *J. Membr. Biol.* **64**, 233–239.